LA-UR-95- 2590

CONF-9511120--1

Los Alamos National Laboratory is operated by the University of California for the United States Department of Energy under contract W-7405-ENG-36

TITLE: **CONSTITUTIVE MODELING USING THE TAYLOR IMPACT TEST**

AUTHOR(S): S(tanley) E. Jones, University of Alabama
Paul J. Maudlin, T-3
J. C. Foster, Eglin AFB

SUBMITTED TO: *Symposium on High Strain Rate Effects on Polymers Metal and Ceramic Matrix Composites and Other Advanced Materials, ASME Congress and Exposition, San Francisco, California, November 14, 1995*

Los Alamos
Los Alamos National Laboratory
Los Alamos, New Mexico 87545

FORM NO. 836 R4
ST. NO. 2629 5/81

CONSTITUTIVE MODELING USING THE TAYLOR IMPACT TEST

S.E. Jones
Department of Mechanical Engineering
University of Alabama
Tuscaloosa, Alabama

Paul J. Maudlin
Theoretical Division
Los Alamos National Laboratory
Los Alamos, New Mexico

J.C. Foster, Jr.
Wright Laboratory
Armament Directorate
Eglin Air Force Base, Florida

ABSTRACT

The Taylor test can be conveniently divided into three fairly distinct stages. The first stage is initial transient behavior after impact characterized by nonlinear plastic wave propagation. The second stage is quasi-steady propagation of the plastic wave front. The duration of this stage is a function of the specimen caliber and material. The final stage is terminal transient behavior, during which most of the deceleration of the undeformed section takes place.

After the initial transient is complete, which varies with the strain at which the plastic wave front propagates, the motion is very well behaved, in the sense that a one-dimensional analysis can be effectively applied. This paper contains such an analysis. The results are supported by an example from which the state of stress for an OFHC copper specimen is deduced.

INTRODUCTION

The motion of Taylor impact specimens has been discussed in some detail by the authors [1–3]. In this series of papers, estimates for plastic wave speed, stress, and other key material properties were given. These estimates were developed using two different viewpoints [1,2] and were verified with a continuum calculation [3]. The purpose of this paper is to introduce a new estimate for the maximum strain-rate after the initial transient. This estimate, along with the equation for stress at constant strain [1-3] for the plastic material, allows us to deduce the state of stress at strain-rates exceeding 10^4/sec. A stress/strain-rate diagram at 10% compressive strain for OFHC copper is included as an example at the end of the paper.

The success of the analysis presented in this paper is based on the observation that the particle velocity u of the material at the plastic wave front is proportional to the current speed of the undeformed section v after the initial transient is over. This means that

$$u = \beta v \tag{1}$$

where β is the constant of proportionality. This hypothesis was first introduced by the authors in [4] without any supporting evidence. Strong supporting evidence for this assumption comes from continuum mechanics code calculations. Figure 1 shows such a calculation for an OFHC copper cylinder, impacting a hardened 4340 steel anvil. The impact velocity is 176 m/s and after the initial transient the relationship between u and v is perfectly linear throughout the period of quasi-steady deformation and the terminal transient. Notice that the slope of the line in Figure 1 corresponds to a value of β approximately 0.85. In [2], this value of corresponds to a strain at the plastic wave front of about 7% in compression.

The notation used in this paper is the same as that used in all of our previous papers, e.g. [4]. For convenience, Figure 2 shows deformed and undeformed specimens. The position of the plastic wave front relative to the fixed anvil face is h. The current undeformed section length is ℓ. The displacement of the back end of the specimen is s, with $\dot{s} = v$. The engineering strain across the plastic wave front is $e = A_0/A - 1$, where A_0 is the original cross-sectional area of the specimen and A is the deformed cross-sectional area.

Conservation of mass (assuming constant density ρ across the plastic wave front) is given by

$$e\dot{\ell} = v - u = (1-\beta)v \,. \tag{2}$$

The equations of motion for the undeformed section ℓ introduced in [1-2] are:

$$\rho \ell \dot{v} = \sigma_0 \tag{3}$$

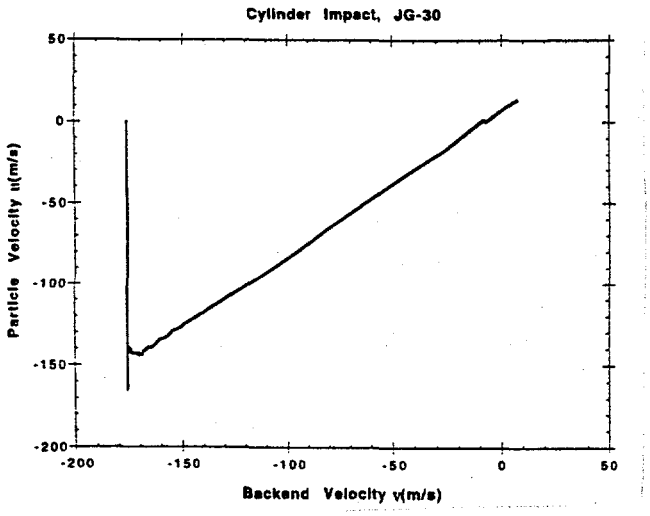

FIGURE 1. The relationship between particle velocity at the plastic wave front, *u*, and undeformed secton velocity, v. Notice that the relationship is completely linear, after a period of initial transient behavior.

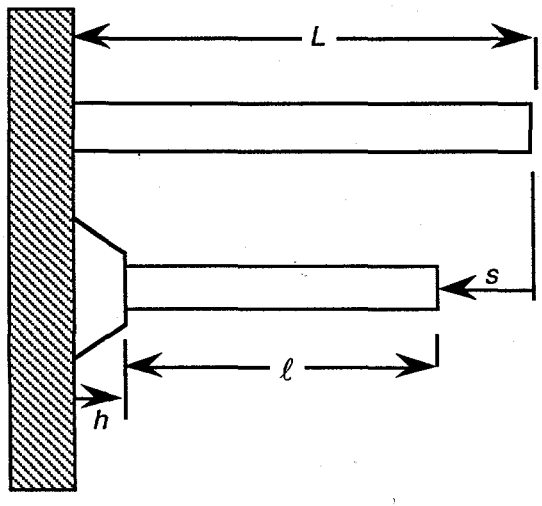

FIGURE 2. A taylor impact specimen of original length *L* undergoing plastic deformation.

and

$$\rho\dot{\ell}(v-u)=\frac{\sigma}{1+e}-\sigma_0\ . \tag{4}$$

In these equations σ_0 is the quasi-static yield stress in compression for the specimen material and σ is the dynamic compressive yield stress. By using equations (1) and (2), we can write equation (4) in the form

$$\sigma=(1+e)\left(\sigma_0+\frac{(1-\beta)^2}{e}\rho v^2\right), \tag{5}$$

which expresses the dynamic yield stress in terms of the quasi-static yield stress and the current velocity, a fact which will be useful later.

EVALUATION OF KEY PARAMETERS

The philosophy behind following a plastic wave of constant strain e has been fairly well documented by the authors [1-3]. In [2], it was shown that post-test measurements of recovered Taylor cylinders could be used to determine the key parameters in the test. Two fundamental relationships were devised from kinematic considerations and a detailed examination of the particle velocity during the initial transient [5]. Without further discussion, these relations are:

$$h_f-\bar{h}=-\left(1+\frac{1-\beta}{e}\right)\left(s_f-\bar{s}\right) \tag{6}$$

and

$$\frac{\bar{h}}{v_0\bar{t}}=\frac{2\beta-1}{3e}-\frac{1+2e}{2e} \tag{7}$$

where $\bar{h}$ is the position of the plastic wave front at the end of the initial transient (see Figure 2). The distance $\bar{s}=v_0\bar{t}$ is the displacement of the undeformed section at the end of the initial transient. The time $\bar{t}$ will vary for differing strains, as will the distance $\bar{h}$. Figure 3, included here with the permission of the authors [6], shows reduced EPIC code calculations from a Taylor cylinder test on OFHC copper. For low strains, $\bar{h}$ is large while $\bar{t}$ is small. For large strains, $\bar{h}$ is small while $\bar{t}$ is large. The distances h_f and s_f can be measured from a recovered specimen for the strain prescribed. The impact velocity v_0 is known from test instrumentation.

For a prescribed, compressive strain e, equations (6) and (7) are a pair of linear algebraic equations for the determination of β and $\bar{h}$. We assume that the transition time $\bar{t}$ is known. Notice that when $\bar{h}$ has been found, $\bar{\ell}$ can be determined from

$$\bar{h}+\bar{\ell}+\bar{s}=L \tag{8}$$

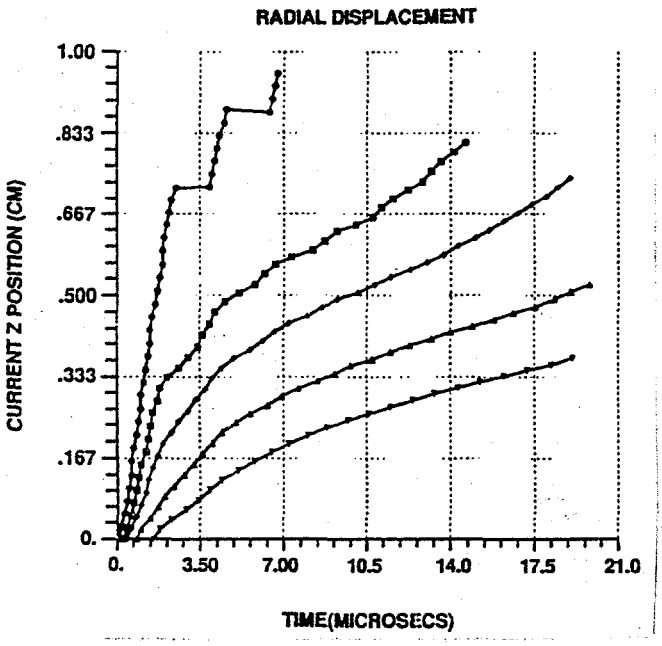

FIGURE 3. EPIC code calculation showing normalized radial displacement $(R-R_0)/R_0$ versus time (included with the permission of the authors [6]). The normalized displacements correspond to 0.002, 0.010, 0.020, 0.050, and 0.100. The highest curve corresponds to the normalized displacement of 0.002 (0.4% compressive strain) and the largest curve corresponds to the normalized displacement of 0.100 (17.4% compressive strain).

which stems from Figure 2. Also, when β has been found, the plastic wave speed can be determined by

$$\dot{h} = -\left(1+\frac{1-\beta}{e}\right)v \tag{9}$$

which is the result of combining

$$\dot{h}+\dot{\ell}+v=0 \tag{10}$$

with equation (2). Reference [2] contains a thorough discussion of these equations and the motivation behind them. A discussion of the post-test measurement technique is also included in this reference.

BEHAVIOR AFTER THE INITIAL TRANSIENT

Equation (3) describes the motion of the undeformed section ℓ during the period of quasi-steady deformation following the initial transient and the terminal transient during which most of the deceleration takes place. Equation (3) can be integrated directly when equation (2) is used to change the variables.

$$\frac{\rho(1-\beta)}{e\sigma_0}vdv=\frac{d\ell}{\ell} \tag{11}$$

Integration of this equation leads to

$$\frac{\rho(1-\beta)}{2e\sigma_0}v^2=\ell n(\ell)+C_1 \tag{12}$$

The constant of integration C_1 can be evaluated with the conditions at the end of the event. In this case,

$$C_1=\frac{\rho(1-\beta)}{2e\sigma_0}v_c^2-\ell n(\ell_f) \tag{13}$$

where ℓ_f is the undeformed section length corresponding to the strain e with which the plastic wave is associated and v_c is the critical velocity of the undeformed section below which deformation at that strain can no longer be sustained. When equations (12) and (13) are combined, we get

$$\ell=\ell_f\ exp\left\{\frac{\rho(1-\beta)}{2e\sigma_0}\left(v^2-v_c^2\right)\right\}, \tag{14}$$

which is the velocity dependent undeformed section length. Notice that the critical velocity v_c can be found from

$$\bar{\ell}=\ell_f\ exp\left\{\frac{\rho(1-\beta)}{2e\sigma_0}\left(v_0^2-v_c^2\right)\right\} \tag{15}$$

because $\bar{\ell}$ can be determined from equation (8).

Equations (3) and (14) are also the source for information about the displacement of the undeformed section, s. Changing the variables and separating them leads to

$$ds=\frac{\rho\ell_f}{\sigma_0}\ exp\left\{\frac{\rho(1-\beta)}{2e\sigma_0}\left(v^2-v_c^2\right)\right\}vdv \tag{16}$$

Integration of this equation gives

$$s+C_2=\frac{e\ell_f}{1-\beta}\ exp\left\{\frac{\rho(1-\beta)}{2e\sigma_0}\left(v^2-v_c^2\right)\right\} \tag{17}$$

The constant of integration can be evaluated from the conditions that exist at the beginning of quasi-steady, plastic wave propagation [4,5],

$$C_2=\frac{e\ell_f}{1-\beta}\ exp\left\{\frac{\rho(1-\beta)}{2e\sigma_0}\left(v_0^2-v_c^2\right)\right\}-\bar{s} \tag{18}$$

and now equation (17) becomes

$$s-\bar{s}=\frac{e\ell_f}{1-\beta}\left[exp\left\{\frac{\rho(1-\beta)}{2e\sigma_0}\left(v^2-v_c^2\right)\right\}-exp\left\{\frac{\rho(1-\beta)}{2e\sigma_0}\left(v_0^2-v_c^2\right)\right\}\right] \tag{19}$$

Notice that at the end of the event when $v = v_c$,

$$s_f - \bar{s} = \frac{e\ell_f}{1-\beta}\left[1 - exp\left\{\frac{\rho(1-\beta)}{2e\sigma_0}\left(v_0^2 - v_c^2\right)\right\}\right], \qquad (20)$$

which relates the total displacement during the quasi-steady and terminal transient stages to the change in velocity.

One useful estimate remains to be found. The terminal time can be obtained from equations (3) and (14) by separating the time and velocity.

$$dt = \frac{\rho\ell}{\sigma_0}\, exp\left\{\frac{\rho(1-\beta)}{2e\sigma_0}\left(v^2 - v_c^2\right)\right\}dv \qquad (21)$$

Integrating this equation between the transition time $\bar{t}$ and the current time t allows us to find

$$t = \bar{t} - \frac{\rho\ell_f}{\sigma_0}\int_v^{v_c} exp\left\{\frac{\rho(1-\beta)}{2e\sigma_0}\left(v^2 - v_c^2\right)\right\}dv \qquad (22)$$

This equation estimates the current time in terms of the current velocity, v.

ESTIMATION OF STRAIN-RATES

The strain-rate is the most difficult physical quantity to estimate in the test. However, for a complete description of the material it is essential. Taylor [7] and Whiffin [8] discussed the difficulties associated with "rate of strain estimation" in their seminal papers. Their estimates are for average strain-rates with which the average yield stress can be associated. There is no strain connected with these quantities.

Taylor's [7] strain-rate estimate is based on uniform deceleration of the undeformed section. If one assumes that dv/dt = const., then it follows that

$$\frac{1}{2}v^2 = \frac{dv}{dt}s + \frac{1}{2}v_0^2 \,. \qquad (23)$$

At the end of the event, this equation can be used to solve for dv/dt.

$$\frac{dv}{dt} = \frac{-\frac{1}{2}v_0^2}{L - L_f} \qquad (24)$$

Separating the variables in this equation and integrating provides us with an estimate for the terminal time, t_f,

$$t_f = \frac{L - L_f}{v_0/2} \,, \qquad (25)$$

at which v = 0.

The post-test geometry of a recovered Taylor cylinder is shown in Figure 4. The average engineering strain in the deformed region of the cylinder is given by

$$\frac{\left(L_f - \ell_f\right) - \left(L - \ell_f\right)}{L - \ell_f} = -\frac{L - L_f}{L - \ell_f} \,. \qquad (26)$$

Using the terminal time estimate given in equation (25), an estimate for the average strain-rate can be found.

$$\dot{e}_{Av} = -\frac{\left(L_f - \ell_f\right)}{L - \ell_f}\frac{\frac{1}{2}v_0}{L - L_f} = -\frac{\frac{1}{2}v_0}{L - \ell_f} \qquad (27)$$

This is Taylor's estimate for the average strain-rate in a Taylor test. Generally, it underestimates the highest rate achieved in the test.

An estimate similar to that of Taylor can be constructed for the present theory. Beginning with equation (23), we modify the result to account for initial transient behavior and find the equivalent of equation (24).

$$\frac{dv}{dt} = -\frac{\frac{1}{2}\left(v_0^2 - v_c^2\right)}{s_f - \bar{s}} \qquad (28)$$

Separating the variables in this equation and integrating leads to the time estimate

$$t_f - \bar{t} = \frac{2\left(s_f - \bar{s}\right)}{v_0 + v_c} \qquad (29)$$

under these conditions, equation (26) becomes

$$\frac{\left(L_f - \ell_f\right) - \left(\bar{\ell} - \ell_f\right)}{\bar{\ell} - \ell_f} = -\frac{\bar{\ell} - L_f}{\bar{\ell} - \ell_f} \qquad (30)$$

Combining equations (29) and (30), we can estimate the average strain-rate for the particular strain in the event.

$$\dot{e}_{Av} = -\frac{\bar{\ell} - L_f}{\bar{\ell} - \ell_f}\,\frac{v_0 + v_c}{2\left(s_f - \bar{s}\right)} \qquad (31)$$

The quantities necessary to make this calculation are all contained in the previous sections. However, the results, like equation (27) are based on uniform deceleration and are typically low.

To improve the strain-rate estimate, we can follow Taylor's reasoning for the current configuration of the specimen. Assuming that the strain behind the plastic wave front is approximately uniform, we can express the average strain-rate as a function of the current position of the rod in the following form.

$$\dot{e} = \frac{-s}{L - \ell}\,\frac{1}{t} \qquad (32)$$

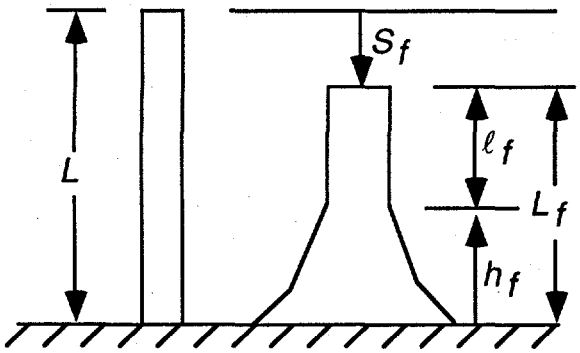

FIGURE 4. Deformed and undeformed taylor cylinders. The nomenclature used to describe the deformed cylinder is shown.

An estimate for the maximum rate achieved in the test after the initial transient can now be easily found.

$$\dot{e}_{\max} = \frac{-\bar{s}}{L-\bar{\ell}}\,\frac{1}{\bar{t}} = \frac{-v_0}{L-\bar{\ell}} \tag{33}$$

It is tempting to use equations (14), (19), and (22) to estimate the strain-rate as a function of velocity and then draw stress/strain-rate diagrams [8] However, because equation (32) utilizes uniform strain behind the plastic wave front, it does not predict the rates very well for large times after the initial transient. The assumption is reasonable when the transition from initial transient behavior to quasi-steady deformation occurs (equation (33)), because the deformation zone is thin.

Conclusion

We conclude this paper with an example intended to clarify the very abbreviated presentation in the previous sections. To accomplish this, data from a Taylor test on OFHC copper [6] is presented in Table 1. A 30 caliber rod impacts a hardened 4340 steel anvil at 176 m/s. The axial position is measured from the undeformed (back) end of the specimen and the associated diameter is given at intervals of 0.050". From these measurements, we can approximate the undeformed section lengths for given strains. For example, if e = –0.10, which corresponds to a diameter of 0.316", then we can use linear interpolation to find ℓ_f = 0.867" = 22.0 mm. For this specimen L = 57.15 mm and L_f = 42.91 mm (See Figure 4). This means that h_f = 20.89 mm and s_f = 14.24 mm. For this impact, $\bar{t}$ = 14 μs is a reasonable choice, and from this estimate $\bar{s} = v_0\bar{t} = 2.46$ mm.

Using the information in the previous paragraph, we can solve equations (6) and (7) for β and $\bar{h}$. The results are: β = 0.768 and $\bar{h}$ = 5.40 mm. It now follows that $\bar{\ell} = L - \bar{h} - \bar{s} = 49.29$ mm.

We are now in a position to estimate the state of stress at 10% compressive strain. Using equation (5) with

TABLE 1

Axial Position (inches)	Rod Diameter (inches)	Axial Position (inches)	Rod Diameter (inches)	Axial Position (inches)	Rod Diameter (inches)
0.000	0.300	0.800	0.308	1.275	0.380
0.050	0.300	0.825	0.310	1.300	0.384
0.100	0.300	0.850	0.315	1.325	0.388
0.150	0.300	0.875	0.318	1.350	0.392
0.200	0.300	0.900	0.321	1.375	0.399
0.250	0.300	0.925	0.324	1.400	0.404
0.300	0.300	0.950	0.327	1.425	0.405
0.350	0.300	0.975	0.333	1.450	0.409
0.400	0.300	1.000	0.337	1.475	0.412
0.450	0.300	1.025	0.342	1.500	0.410
0.500	0.300	1.050	0.346	1.525	0.409
0.550	0.300	1.075	0.350	1.550	0.409
0.600	0.301	1.100	0.353	1.575	0.417
0.650	0.302	1.125	0.358	1.600	0.440
0.675	0.303	1.150	0.361	1.625	0.476
0.700	0.304	1.175	0.365	1.650	0.511
0.725	0.304	1.200	0.369	1.675	0.535
0.750	0.306	1.225	0.373	1.687	0.541
0.775	0.308	1.250	0.376		

σ_0 = –300 MPa, we find σ = –404 MPa. From equation (33) we find that this stress corresponds to a strain-rate of $-2.24\text{x}10^4\ \text{s}^{-1}$. These estimates are all very reasonable and consistent with our earlier efforts [2, 3].

The one-dimensional analysis contained in this paper has been successfully applied to many Taylor specimens. Although only one example has been included, it is clear that data at other strains can be obtained using the same analysis. By varying the impact speed, other strain-rates can be achieved and the stress/strain-rate diagram can be constructed at constant strain. Some of these diagrams will be reported later.

It is possible to develop the constitutive behavior for the specimen material parametrically in terms of the velocity v [9]. Future efforts will concentrate on improving the estimate for velocity dependent strain-rate.

REFERENCES

1. Foster, J.C., Jr., P.J. Maudlin, and S.E. Jones, 1995, "A Continiuum Analysis of Plastic Wave Propagation in the Taylor Test," Proceedings of the 1995 APS Topical Conference on Shock Compression of Condensed Matter, Seattle, WA.

2. Jones, S.E., P.J. Maudlin, J.C. Foster, Jr., and M. Kazmeir, 1994, "On the Taylor Test, Part II: An Engineering Analysis of Plastic Wave Propagation," Los Alamos National Laboratory report LA-12845-MS.

3. Maudlin, P.J., J.C. Foster, Jr., and S.E. Jones, 1994, "On the Taylor Test, Part III: A Continuum Mechanics Code Analysis of Steady Plastic Wave Propagation," Los Alamos National Laboratory report LA-12836-MS.

4. Jones, S.E., P.P. Gillis, J.C. Foster, Jr., and L.L. Wilson, 1991, "A One-Dimensional Two-Phase Flow Model for Taylor Impact Specimens," *J. Engr. Mat'ls. Tech. Trans. ASME*, Vol. 113, p. 228.

5. Jones, S.E., P.J. Maudlin, P.P. Gillis, and J.C. Foster, Jr., 1992, "An Analytical Interpretation of High Strain

Rate Material Behavior During Early Time Plastic Deformation in the Taylor Impact Test," Proceedings of the ASME Computers in Engineering Conference, San Francisco, CA.

6. Wilson, L.L., J.W. House, and M.E. Nixon, 1989, "Time Resolvable Deformation from the Cylinder Impact Test," AFATL-89-76, Air Force Armament Laboratory, Eglin AFB.

7. Taylor, G.I., 1948, "The Use of Flat-Ended Projectiled for Determining Dynamic Yield Stress I Theoretical Considerations," *Proc. Roy. Soc. London*, Series A, Vol. 194, p. 289.

8. Whiffin, A.C., 1948, "The Use of Flat-Ended Projectiles for Determining Dynamic Yield Stress II. Tests on Various Metallic Materials," Vol. 194, p. 300.

9. Jones, S.E., David Allen, Scott Sharp, and Joseph C. Foster, Jr., 1994, "A Parametric Representation for the Constitutive Properties of Metals at High Strain-Rates," Proceedings of the 14th World Congress on Computational and Applied Mathematics, Atlanta, GA, p. 749.

DISCLAIMER